

Angular Momentum in Subbarrier Fusion: Isomer Ratio Measurements and a Global Analysis *

D.E. DiGregorio +, K.T. Lesko, B.A. Harmon, E.B. Norman,
J. Pouliot, B. Sur, Y.D. Chan, and R.G. Stokstad

Nuclear Science Division, Lawrence Berkeley Laboratory,
1 Cyclotron Road, Berkeley, CA 94720

LBL--29135

Abstract

DE90 015721

We have measured the ratio of the isomer to ground-state yields of ^{137}Ce produced in the fusion reactions $^{128}\text{Te}(^{12}\text{C},3n)$, $^{133}\text{Cs}(^7\text{Li},3n)$, $^{136}\text{Ba}(^3\text{He},2n)$, $^{136}\text{Ba}(^4\text{He},3n)$, and $^{137}\text{Ba}(^3\text{He},3n)$, from energies above the Coulomb barrier to energies typically 20-30 % below the barrier by observing the delayed x- and γ -ray emission. We deduce the average angular momentum, $\langle J \rangle$, from the measured isomer ratios with a statistical model. In the first three reactions we observe that the values of $\langle J \rangle$ exhibit the behavior predicted for low energies and the expected variation with the reduced mass of the entrance channel. We analyze these data and the associated cross sections with a barrier penetration model that includes the coupling of inelastic channels. Measurements of average angular momenta and cross sections made on other systems using the γ -multiplicity and fission-fragment angular correlation techniques are then analyzed in a similar way with this model. The discrepancies with theory for the γ -multiplicity data show correlations in cross section and angular momentum that suggest a valid model can be found. The measurements of angular momentum using the fission fragment angular correlation technique, however, do not appear reconcilable with the energy dependence of the cross sections. This systematic overview suggests, in particular, that our current understanding of the relationship of angular momentum and anisotropy in fission fragment angular correlations is incomplete.

I. Introduction

The measured cross sections for the fusion of heavy ions at energies near and below the Coulomb barrier can be orders of magnitude larger than the predictions of the one-dimensional barrier penetration model [Be 85, St 86, Si 88]. Theoretical studies of these enhancements have revealed the important role played by the nuclear structure of the colliding nuclei. Additional and complementary information has been obtained by measuring the moments of the angular momentum distributions leading to fusion with three different

*Supported by U.S. Dept. of Energy under Contract No. DE-AC03-76SF00098.

+Permanent address: Departamento de Fisica-TANDAR, Comision Nacional de Energia Atomica, 1429 Buenos Aires, Argentina and CONICET.

MASTER

techniques: γ -multiplicity [Va 83, Gi 85, Ha 85, No 85, Fi 86, Ha 89, Du 90], fission fragment angular distributions [Ba 85a, Va 86, Mu 86, Vu 86, Zh 89] and very recently by our measurements of isomer ratios [St 89, Di 90a]. With the latter method it was possible to observe the predicted energy-independent lower limit for $\langle l \rangle$ [St 89]. Measurements of the cross sections, $\sigma(E)$, and the deduction of average angular momenta, $\langle l \rangle$, by the isomer method provide an independent experimental approach to the problem that the theoretical values of $\langle l \rangle$ disagree with those deduced from fission fragment angular distributions and, sometimes, from gamma-ray multiplicities. This discrepancy has been an important and perhaps the central problem in studies of subbarrier fusion for several years [Da 86, Mu 86, Va 86, Es 87]. Theoretical models [e.g., Da 85, Da 86, Es 87] must account for both the measured subbarrier $\sigma(E)$ and the $\langle l \rangle$. This double requirement places a strong constraint on a model, because within a given model, the angular momentum distribution and the energy dependence of the cross section are intimately related.

II. Experiment and results

The ground ($J^\pi = 3/2^+$, $t_{1/2} = 9.0$ h) and isomeric ($11/2^-$, 34.4 h) states in ^{137}Ce (see Fig. 1) were populated by the reactions $^{128}\text{Te}(^{12}\text{C}, 3n)$, $^{133}\text{Cs}(^7\text{Li}, 3n)$, $^{136}\text{Ba}(^3\text{He}, 2n)$, $^{137}\text{Ba}(^3\text{He}, 3n)$, and $^{136}\text{Ba}(^4\text{He}, 3n)$, using beams from the LBL 88-Inch Cyclotron. Targets and carbon and gold catcher foils were arranged in a stack to permit irradiations at several energies in a single bombardment. After a bombardment of typically eight hours at intensities of ≤ 100 ena, the x and γ -radiations from the target/catcher foils were counted off-line for several days using germanium detectors. The x and γ -ray spectra were accumulated in one hour intervals, and recorded automatically for additional analysis. The absolute fusion cross sections and isomer ratios were determined by fitting the time dependence of the characteristic x and γ -ray emissions following the bombardment. Typical decay curves for a small and a large isomer ratio are shown in Fig. 1.

The experimental results for the isomer ratios of $^{12}\text{C} + ^{128}\text{Te}$, $^7\text{Li} + ^{133}\text{Cs}$, and $^3\text{He} + ^{136}\text{Ba}$ are shown in Fig. 2 as a function of the difference of the center-of-mass energy and the Coulomb barrier. The isomer ratio, R , decreases rapidly as the bombarding energy is lowered and approaches the barrier. However, for energies well below the barrier the change in R with bombarding energy is much slower, and the isomer ratio for each reaction becomes nearly constant. The approximate constancy of R indicates that the ratio of cross sections for fusion proceeding through partial waves above and below some critical value has an approximately constant, energy independent value. Assuming (as is predicted by all fusion models) that the individual partial wave cross sections vary smoothly with energy, this result implies a constant average angular momentum for fusion.

Indeed, the observed dependence of R on the bombarding energy, and on the masses of the projectile and target indicates that the isomer ratio is a measure of the average angular momentum leading to fusion, and that this angular momentum approaches a constant at energies well below the barrier. A quantitative justification of this conclusion will be given in the sections III and IV where model calculations are discussed.

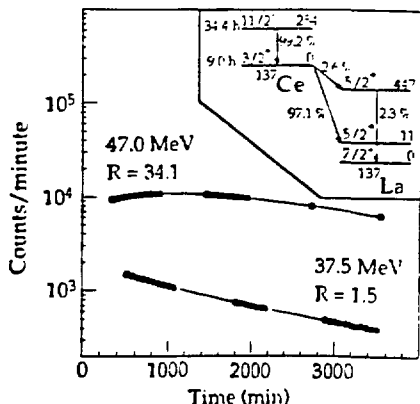


Fig. 1. The time dependence of the summed Ce and La K x-rays obtained for $^{12}\text{C} + ^{128}\text{Te}$ at $E_{\text{c.m.}} = 37.5$ and 47 MeV. The curves are fits to the data and result in the indicated values for the isomer ratio.

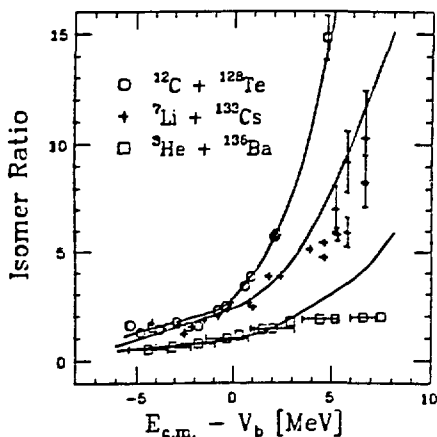


Fig. 2. The experimental excitation functions of the isomer ratio for the systems $^{128}\text{Te} + ^{12}\text{C}$ (open circles), $^{133}\text{Cs} + ^7\text{Li}$ (small stars), and $^{136}\text{Ba} + ^3\text{He}$ (open squares). The solid curves are the model predictions. The energy of the entrance channel is expressed in terms of the difference of the center-of-mass energy and the Coulomb barrier.

The measured isomer ratios and absolute cross sections for the $3n$ channel for $^{12}\text{C} + ^{128}\text{Te}$ are shown in Fig. 3. It should be pointed out that the values of the cross sections for $^{12}\text{C} + ^{128}\text{Te}$ shown in Fig. 2 of Ref. [St 89] are too low by a factor of 1.9. This error arose from a beam integration problem. The conclusions of Ref. [St 89] however, are not affected

by this change in absolute normalization of the cross sections.

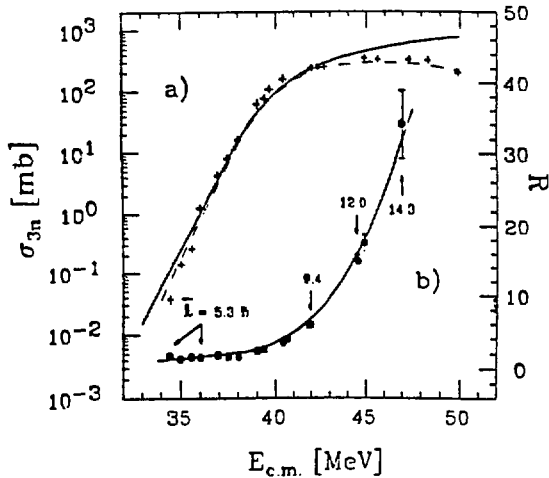


Fig. 3. (a) The measured $3n$ fusion cross sections for the $^{12}\text{C} + ^{128}\text{Te} = ^{137}\text{Ce} + 3n$ reaction. The full curve is a calculation of the total fusion cross section as described in the text. The dashed curve shows the prediction for the $3n$ cross section, obtained with use of the predicted xn distributions. (b) The experimental isomer ratio. The full curve is a prediction based on the angular momentum distribution predicted by CCFUS and a statistical-decay calculation made with the code PACE. The predicted average angular momentum is indicated for selected bombarding energies.

III. Quantitative comparison of predictions with experiments

In order to compare theory and experiment it is necessary to relate a total cross section and a distribution of angular momentum for ^{140}Ce (or ^{139}Ce for one reaction) in the entrance channel to the $3n$ (or $2n$) cross sections and isomer ratios for ^{137}Ce . This is done by means of a statistical model, which for a given excitation energy and angular momentum in the compound nucleus gives the probability that three (two) neutrons will be evaporated and that the subsequent γ -ray cascade will populate the isomer or the ground state. Combined with a model for fusion, which gives the total cross section and the initial distribution of angular momentum, the statistical model makes it possible to compare theory and experiment directly in terms of the *measured quantities*. The partial wave cross sections were calculated with the simplified coupled channels computer code CCFUS of Dasso and Landowne [Da 85], which employs the parabolic barrier approximation. Known electromagnetic coupling matrix elements in the projectile and target nuclei were included, and the parameters describing the nuclear-plus-Coulomb potential were obtained by scaling the values determined experimentally for $^{16}\text{O} + \text{Sm}$ [Di 86]. Slight adjustments (less than 1.2%) were made for ^{12}C

+ ^{128}Te . The statistical decay of the compound nucleus was calculated using the computer code PACE [Ga 80], which included E1 and E2 γ -ray decay in competition with neutron emission. The input parameters used in this calculation were taken from [Di 89] and are those that reproduce the measured x - n distributions for the fusion of ^{16}O with the isotopes of Sm [Di 89, St 80]. Known states in ^{137}Ce below 2 MeV having spins of 1/2, 3/2, and 5/2, as well as the band built on the isomeric level were included in the calculation [Pe 83]. Since states having spins of 7/2 and 9/2 must also be present below 2 MeV, they were inserted in the level scheme at random energies according to an estimated density. The calculations presented in this work used the rigid body moments of inertia calculated by Sierk [Si 86] for the spin cutoff factor in the level density formula of Gilbert and Cameron [Gi 65]. The remaining input parameters, such as the optical model parameters for transmission coefficients, were as described in Ref. [Ga 80]. Whenever the ground state spin of an entrance channel nucleus was non-zero (^7Li : 3/2, ^{133}Cs : 7/2, ^3He : 1/2), the distribution of the total spin in the compound nucleus, $\mathbf{J} = \mathbf{l} + \mathbf{S}_1 + \mathbf{S}_2$, was computed and used in the evaporation calculation. A detailed discussion of the statistical model calculations, their sensitivity to variation of input parameters are given elsewhere [Di 90a].

The predicted total fusion cross sections (full line) and those for the $3n$ channel alone (dashed line) are shown in Fig. 3 (a). These predictions agree well with the experimental data from above the barrier down to about 35 MeV. The calculated isomer ratios for $^{12}\text{C} + ^{128}\text{Te}$, $^7\text{Li} + ^{133}\text{Cs}$, and $^3\text{He} + ^{136}\text{Ba}$ are shown in Fig. 2. Figure 3 (b) compares the calculated and measured isomer ratios for $^{12}\text{C} + ^{128}\text{Te}$ as a function of the center-of-mass energy, along with the experimental results. The agreement of the calculations with the data is very good below the barrier.

We find that the isomer ratio has nearly the same value (≈ 1.5) for both the $^{12}\text{C} + ^{128}\text{Te}$ and $^7\text{Li} + ^{133}\text{Cs}$ systems, even though the average orbital angular momentum for a ^7Li projectile is less than for ^{12}C . This is a consequence of the spin coupling mentioned above, which introduces an extra spin angular momentum $\mathbf{S} = 3/2 + 7/2$ in the case of $^7\text{Li} + ^{133}\text{Cs}$. The intrinsic spin 1/2 of ^3He nucleus does not significantly affect the predicted value of R (≈ 0.8) for $^3\text{He} + ^{136}\text{Ba}$. Thus the predictions of CCFUS for $\langle l \rangle$ at low energies and the variation of $\langle l \rangle$ with the reduced mass below the barrier are consistent with the measured values of R , as shown in Fig. 2.

IV. Determination of the average angular momentum from the isomer ratio

The preceding section has shown that the distribution of angular momentum predicted by a barrier penetration model is consistent with the experimentally observed isomer ratio. In this section we want to turn the problem around and, starting with the experimental value of the isomer ratio, determine the average angular momentum without particular reference to a model for fusion. Our determination will be model independent to the extent that there is a one-to-one correspondence between the isomer ratio and the average angular momentum, i.e., that the deduced average is independent of the other, and unknown, moments of the distribution. In this process of relating the average angular momentum to the isomer ratio, we regard the statistical decay calculation, with the parameters determined as described in the

preceding section and in Ref. [Di 90a], as given.

In these calculations we used a Fermi function for the shape of the initial spin distribution with fixed ΔI and variable l_0 . This procedure was repeated for all systems studied. The results for $^{12}\text{C} + ^{128}\text{Te}$ are given in Fig. 4. A smooth curve was drawn through the experimental values of the isomer ratios (right ordinate). Values from this curve were then converted into angular momentum at selected energies (left ordinate). The dashed line represents the average angular momentum predicted by CCFUS. Note the constant value of the angular momentum obtained at the lowest energies and the agreement between the deduced and the predicted values of $\langle J \rangle$.

Fig. 5 displays and summarizes the deduced values of $\langle J \rangle$ as a function of the excitation energy in the compound nucleus (^{140}Ce (or ^{139}Ce for one reaction) for all systems studied in the present work.

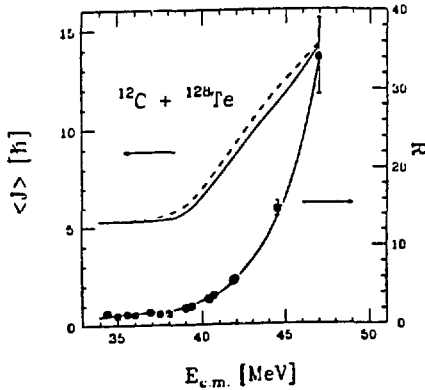


Fig. 4. The observed isomer ratio (right ordinate) and the deduced $\langle J \rangle$ (left ordinate) for the system $^{12}\text{C} + ^{128}\text{Te}$. The dashed line represents the $\langle J \rangle$ predicted by CCFUS.

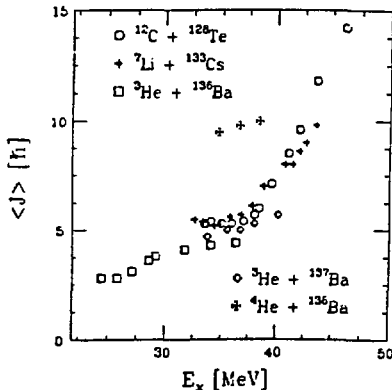


Fig. 5. Experimental average angular momentum as a function of the excitation energy in the compound nucleus for all the systems studied in this work.

V. Systematic Analysis of Average Angular Momenta and Cross Sections in Subbarrier Fusion

We have investigated, following Ref. [Va 88], all the present available data on the first and second moments of the spin distributions leading to fusion and compare them with the *same* theory. In addition, we analyzed the corresponding experimental cross section since the starting point in the analysis of the fusion data should be to understand the excitation functions. The same coupled-channel code describe above, CCFUS, has been used to perform all model calculations. We present the analysis for fourteen different systems: $^3\text{He} + ^{136}\text{Ba}$ [Di 90a], $^3\text{He} + ^{137}\text{Ba}$ [Di 90a], $^4\text{He} + ^{136}\text{Ba}$ [Di 90a], $^{12}\text{C} + ^{128}\text{Te}$ [St 89, Di 90a], $^{16}\text{O} + ^{144}\text{Nd}$ [Ha 85, Du 90], $^{16}\text{O} + ^{154}\text{Sm}$ [Va 83, Gi 85, Va 88], $^{28}\text{Si} + ^{154}\text{Sm}$ [Ch 90], $^{64}\text{Ni} + ^{96}\text{Zr}$ [Ha 85], $^{80}\text{Se} + ^{80}\text{Se}$ [Ha 85], $^{64}\text{Ni} + ^{100}\text{Mo}$ [Ha 89], $^{16}\text{O} + ^{208}\text{Pb}$ [Ba 85a, Vu 86, Mu 86], $^{12}\text{C} + ^{236}\text{U}$ [Va 86, Mu 86], $^{16}\text{O} + ^{232}\text{Th}$ [Va 86, Mu 86], and $^{19}\text{F} + ^{232}\text{Th}$ [Zh 89]. For all these systems, the fusion cross sections and the first or second moments of their σ_1 have been measured at different bombarding energies by one of the three methods. For a few systems: $^{12}\text{C} + ^{128}\text{Te}$ [Di 90b], $^{16}\text{O} + ^{144}\text{Nd}$ [Di 90c], $^{16}\text{O} + ^{154}\text{Sm}$ [St 80] and $^{28}\text{Si} + ^{154}\text{Sm}$ [Gi 89], fusion excitation functions have been measured in independent experiments.

Fig. 6 (a) displays the ratio of the experimental fusion cross section, σ_{exp} , to the theoretical value, σ_{theo} , (upper frame) and the ratio of the experimental $\langle l \rangle_{\text{exp}}$ value to the theoretical $\langle l \rangle_{\text{theo}}$ value (lower frame) as a function of the ratio of the bombarding energy to the Coulomb barrier, for the data obtained from the isomer ratio measurements. Note that the cross sections and the average angular momenta for $^{12}\text{C} + ^{128}\text{Te}$, $^3\text{He} + ^{136}\text{Ba}$, $^3\text{He} + ^{137}\text{Ba}$ and $^4\text{He} + ^{136}\text{Ba}$ are consistent with the theoretical expectations at bombarding energies above and well below the barrier.

Fig. 6(b) shows a similar comparison for data obtained from γ -ray multiplicity measurements. For the systems $^{28}\text{Si} + ^{154}\text{Sm}$, $^{16}\text{O} + ^{154}\text{Sm}$ and $^{16}\text{O} + ^{144}\text{Nd}$, both the experimental cross sections and the experimental $\langle l \rangle$ values are well described by the CCFUS calculations. On the other hand, when the theory underestimates the cross section for $^{64}\text{Ni} + ^{100}\text{Mo}$ it also underestimates the average angular momentum. More precisely, it is the slope of the cross sections (the logarithmic derivative) that the theory overestimates. This corresponds to an underestimate of the angular momentum, which is also observed. (If the barrier can be approximated by a parabolic shape, then the mean square angular momentum and the energy dependence of the cross section are related by $\langle l^2 \rangle = (2 \mu R_b^2 / \hbar^2) / (d \ln(\sigma_f(E)) / dE)$ at $E \ll V_b$) Thus, the deviations of theory with experiment are in the *same direction* for both cross sections and angular momenta. Halbert et al. have obtained a better fit to the cross sections and the angular momentum by increasing the strength of the coupling for all the inelastic channels by a factor of 1.5 [Ha 89]. Note that there is also a discrepancy between data and theory in the $\langle l \rangle$ values for $^{80}\text{Se} + ^{80}\text{Se}$ at energies below the barrier. Although the corresponding cross sections do not show a clear deviation from theory, it is necessary to point out that relative cross sections were reported in Ref. [No 85], and therefore, in the present analysis have been arbitrarily normalized to the theory at bombarding

energies above the barrier. In any case, it is apparent from this comparison that theory fails to satisfactorily describe the angular momentum and the cross sections at energies below the barrier for the more symmetric systems.

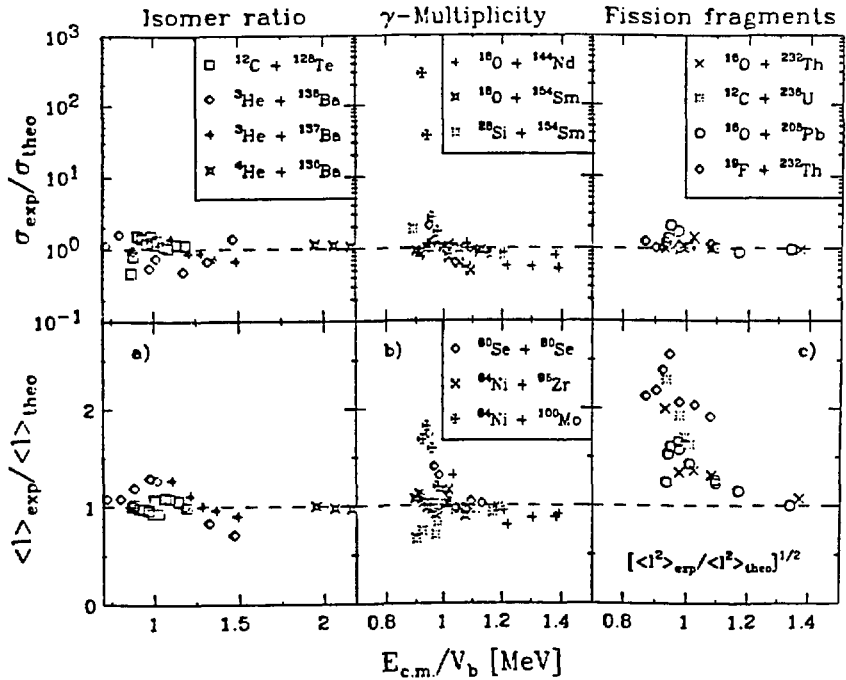


Fig. 6. Comparison of ratios of experimental to theoretical cross sections and average angular momenta as a function of ratio of bombarding energy to the Coulomb barrier.

The comparison between theory and data for the analysis of fission fragment angular distributions is shown in Fig. 6 (c). In this case we have plotted the ratio of the root-mean-square values, $\langle l^2 \rangle^{1/2}$, rather than the mean values. As it was pointed out by Vandebosch [Va 88], the ratios of the mean and the root-mean-square values are not very different for plausible σ_1 . For $^{12}C + ^{236}U$, $^{16}O + ^{232}Th$ and $^{16}O + ^{208}Pb$ the experimental $\langle l^2 \rangle$ values are those obtained in Ref. [Va 86, Mu 86]. Following their approach we have determined the $\langle l^2 \rangle$ values for $^{19}F + ^{232}Th$ from the data of Ref. [Zh 89] by extracting K_0^2 from the prediction of J_0/J_{eff} given by the diffuse surface liquid drop model of Sierk [Si 86]. As one can observe in Fig. 6(c) while the experimental cross sections are well reproduced by the CCFUS calculations, the experimental root-mean-square values significantly deviate from theory at energies around and below the barrier for all the systems. Given that the model reproduces the slope of the cross sections, it is hard to see how it could be so very wrong on the angular momentum. On the other hand, if we follow the arguments of Refs. [Da 86, Es 87], we can take the predicted $\langle l^2 \rangle$ values as a given from the theory (CCFUS) and thus

extract values of K_0^2 from the measured anisotropies for $^{12}\text{C} + ^{236}\text{U}$, $^{16}\text{O} + ^{232}\text{Th}$ and $^{16}\text{O} + ^{208}\text{Pb}$ as was done in Ref. [Zh 89] for $^{19}\text{F} + ^{232}\text{Th}$. In this case we obtain values of K_0 which are a factor of 2-3 larger than those determined by using Sierk's model [Si 86]. Thus, the present analysis shows that our current understanding of the measured fission fragment angular distribution in terms of the available theory (standard transition-state model, coupled-channel calculations and diffuse surface liquid drop model) is incomplete. Since the prediction of the fusion cross sections for projectiles such as ^4He , ^{12}C , and ^{16}O is generally satisfactory, and the comparison with the deduced average angular momenta fails for the case of fission fragment angular correlations, we suspect that the problem is in the deduction of angular momenta from fission anisotropies. Indeed, the question of when and how the distribution of angular momenta projected along the symmetry axis is determined and fixed as the fissioning nucleus proceeds from saddle to scission is a topic still under discussion [Bo 84, Ba 85b, Ro 84].

VI. Summary

We have deduced the average angular momentum, $\langle J \rangle$, from the experimental isomer ratio with a statistical model. The values of $\langle J \rangle$ thus obtained exhibit the predicted behavior of the average angular momentum at low energies and the expected variation with the reduced mass of the entrance channel. The cross sections below the barrier are also explained in this analysis. In addition, we have also analyzed all the existing data on the first or second moments of the spin distributions leading to fusion along with the corresponding experimental cross sections and compared them with the *same* theory. A fairly good agreement was found between the theory and the data obtained from isomer ratio measurements and gamma-ray multiplicity for all the systems with the exception of the more symmetric ones, $^{64}\text{Ni} + ^{100}\text{Mo}$ and less clearly $^{80}\text{Se} + ^{80}\text{Se}$. In these cases when the theory over estimates the logarithmic derivative of the cross section it also underestimates the angular momentum. And finally, the experimental fission-fusion cross sections show very good agreement with theory while showing a large discrepancy in the angular momenta. The present systematic overview suggests that the origin of the discrepancy may lie in the deduction of the angular momentum from the measured fission fragment distributions.

References:

- [Ba 85a] Back B.B., et al., Phys. Rev. C32, 195 (1985)
- [Ba 85b] Back B.B., Phys. Rev. C31, 2140 (1985)
- [Be 85] Beckerman M., Phys. Rep. B129, 145 (1985).
- [Bo 84] Bond P.D., Phys. Rev. Lett., 414 (1984)
- [Ch 90] Charlop A.W., et al., to be published.
- [Da 85] Dasso C.H. and Landowne S., Phys. Rev. C32, 1094 (1985).
- [Da 86] Dasso C.H., et al., Phys. Rev. Lett. 57, 1498 (1986).
- [Da 87] Dasso C.H. and Landowne S., Phys. Lett. B183, 141 (1987); Comp. Phys. Comm. 46, 187 (1987).
- [Di 86] DiGregorio D.E., et al., Phys. Lett. B176, 322 (1986).

- [Di 89] DiGregorio D.E., et al., Phys. Rev. C39, 516 (1989).
[Di 90a] DiGregorio D.E., et al., submitted to Phys. Rev. C.
[Di 90b] DiGregorio D.E., et al., to be published.
[Di 90c] diTada M., et al., to be published.
[Du 90] Duchene G., et al., to be published.
[Es 87] Esbensen H. and Landowne S., Nucl. Phys. A467, 136 (1987).
[Fi 86] Fischer R.D., et al., Phys. Lett B171, 33 (1986).
[Ga 80] Gavron A., Phys. Rev. C21, 230 (1980).
[Gi 65] Gilbert A. and Cameron A.G.W., Can. J. Phys. 43, 1446 (1965).
[Gi 85] Gil S., et al., Phys. Rev. C31, 1752 (1985).
[Gi 89] Gil S., et al., Proc. on the XII Workshop on Nuclear Physics, Iguazu Falls, Argentina, 1989, World Scientific Publishing Co, (to be published).
[Ha 85] Haas B., et al., Rev. Lett. 54, 398 (1985).
[Ha 89] Halbert M.L., et al., Phys. Rev. C40, 2558 (1989).
[Mu 86] Murakami T., et al., Phys. Rev. C34, 1353 (1986).
[No 85] Nolan P.J., et al., Phys. Rev. Lett. 54, 2211 (1985).
[Pe 83] Peker L.K., Nucl. Dat. Sheets. 38, 87 (1983); Mueller-Veggian M., et al., Nucl. Phys. A304, 1 (1978).
[Ro 84] Rossner, H.H., et al., Phys. Rev. Lett., 38 (1984).
[Si 86] Sierk A., Phys. Rev. C33, 2039 (1986).
[Si 88] Signorini C., et al., ed., Proceedings of Symposium on Heavy Ion Interactions around the Coulomb Barrier, Legnaro, Italy, June 1988, Lecture Notes in Physics Vol. 317, (Springer-Verlag, 1988).
[St 86] Steadman S.G. and Rhodes-Brown M.J., Ann. Rev. Nucl. Part. Sci. 36, 649 (1986).
[St 80] Stokstad R.G., et al., Phys. Rev. Lett. 41, 465 (1978); Phys. Rev. C21, 2427 (1980).
[St 89] Stokstad R.G., et al., Phys. Rev. Lett. 62, 399 (1989).
[Va 83] Vandenbosch R., et al., Phys. Rev. C28, 1161 (1983).
[Va 86] Vandenbosch R., et al., Phys. Rev. Lett. 56, 1234 (1986); Phys. Rev. Lett. 57, 1499 (1986).
[Va 88] Vandenbosch R., Proceedings of Symposium on Heavy Ion Interactions around the Coulomb Barrier, Legnaro, Italy, June 1988, edited by C. Signorini et al., Lecture Notes in Physics Vol. 317, 157 (Springer-Verlag, 1988).
[Vu 86] Vulgaris E., et al., Phys. Rev. C33, 2017 (1986).
[Zh 89] Zhang H., et al., Phys. Lett. B218, 133 (1989).

DISCLAIMER

This report was prepared as an account of work sponsored by an agency of the United States Government. Neither the United States Government nor any agency thereof, nor any of their employees, makes any warranty, express or implied, or assumes any legal liability or responsibility for the accuracy, completeness, or usefulness of any information, apparatus, product, or process disclosed, or represents that its use would not infringe privately owned rights. Reference herein to any specific commercial product, process, or service by trade name, trademark, manufacturer, or otherwise does not necessarily constitute or imply its endorsement, recommendation, or favoring by the United States Government or any agency thereof. The views and opinions of authors expressed herein do not necessarily state or reflect those of the United States Government or any agency thereof.